Available online at www.sciencedirect.com

ScienceDirect

Journal of Bionic Engineering 6 (2009) 350–356

Applying Methods from Differential Geometry to Devise Stable and Persistent Air Layers Attached to Objects Immersed in Water

Wilfried Konrad[1], Christian Apeltauer[1], Jörg Frauendiener[2,3], Wilhelm Barthlott[4], Anita Roth-Nebelsick[1,5]

1. *Institute for Geosciences*, *University of Tübingen*, *D*-72076 *Tübingen*, *Germany*
2. *Department of Mathematics and Statistics*, *University of Otago*, *Dunedin* 9054, *New Zealand*
3. *Centre of Mathematics for Applications*, *University of Oslo*, *NO*-0317 *Oslo*, *Norway*
4. *Nees Institute for Biodiversity of Plants*, *University of Bonn*, *D*-53115 *Bonn*, *Germany*
5. *State Museum of Natural History Stuttgart*, *Rosenstein* 1, *D*-70191 *Stuttgart*, *Germany*

Abstract

We describe a few mathematical tools which allow to investigate whether air-water interfaces exist (under prescribed conditions) and are mechanically stable and temporally persistent. In terms of physics, air-water interfaces are governed by the Young-Laplace equation. Mathematically they are surfaces of constant mean curvature which represent solutions of a nonlinear elliptic partial differential equation. Although explicit solutions of this equation can be obtained only in very special cases, it is – under moderately special circumstances – possible to establish the existence of a solution without actually solving the differential equation. We also derive criteria for mechanical stability and temporal persistence of an air layer. Furthermore we calculate the lifetime of a non-persistent air layer. Finally, we apply these tools to two examples which exhibit the symmetries of 2D lattices. These examples can be viewed as abstractions of the biological model represented by the aquatic fern *Salvinia*.

Keywords: interfaces, air layers, differential geometry, stability, persistence, *Salvinia*

doi: 10.1016/S1672-6529(08)60133-X

1 Introduction

Air-water interfaces are important for many applications. The behaviour of air-water interfaces is dictated by their shape, mechanical stability and temporal persistence. These features of air-water interfaces (resp. of the air layers enclosed by them) depend on the surface geometry and chemical properties of the object to which they are attached, on the hydrostatical and hydrodynamic pressures acting upon the interface, and on the air content of the surrounding water which continuously exchanges air molecules with the air layer held by the object.

1.1 Existence and shape

The forces acting upon an interface (resp. the air layer enclosed by it) can settle to an equilibrium only if the Young-Laplace-Equation[1],

$$p_a = p_w + 2\sigma H\,, \tag{1}$$

is compatible with (i) the geometry of the boundary between air-water interface and the solid to which it is attached and (ii) the contact angle between interface and solid object. p_a and p_w denote air and water pressure, respectively, on the two sides of the interface, and σ the surface tension. H is the mean curvature of the interface (for a sphere of radius R, $H = 1/R$).

Characterising the interface by the function $u(x,y)$ (see Fig. 1) the mean curvature can be written more explicitly

$$2H = -\frac{(1+u_x^{\,2})u_{yy} - 2u_x u_y u_{xy} + (1+u_y^{\,2})u_{xx}}{(1+u_x^{\,2}+u_y^{\,2})^{3/2}}\,. \tag{2}$$

If the pressure difference $p_a - p_w$ across the interface is a constant for all points of the interface, Eq. (1) implies that the mean curvature H is a constant, too. If so, Eq. (2)

Corresponding author: Wilfried Konrad
E-mail: wilfried.konrad@uni-tuebingen.de

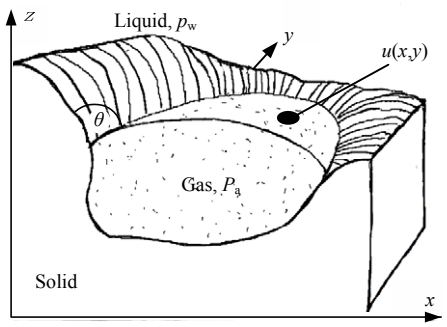

Fig. 1 The shape of the interface is described by giving the distance $u(x,y)$ (measured parallel to the z-axis) between xy-plane and interface for every point (x,y) on the xy-plane. p_a and p_w denote air and water pressure, respectively, on the two sides of the interface, and θ the contact angle.

takes the form of a nonlinear elliptic partial differential equation whose solutions $u(x,y)$ represent surfaces of constant mean curvature ("cmc-surfaces"). Eq. (2) is completed by boundary conditions, usually a prescription of (i) the shape of the contact line between air-water interface and solid and (ii) the contact angle θ between interface and solid object. There is, however, no guarantee that solutions of Eq. (2) exist which are compatible with arbitrary contact angles and arbitrarily shaped boundary geometries.

1.2 Mechanical stability

With regard to many applications, an air layer around an object is useful only if the air-water interface returns to its equilibrium position after a (small) perturbation. Both the surface geometry of the object to which the air-water interface is attached and the contact angle are essential for the stability of an interface. Upon Taylor expansion of Young-Laplace-Equation and Gas-Equation around a point of mechanical equilibrium, it turns out that the quantity

$$\Psi = \left[\frac{p_a}{V_a} + 2\sigma \frac{dH}{dV_a} \right]_0 , \qquad (3)$$

indicates whether a mechanical equilibrium is stable ($\Psi > 0$) or not ($\Psi < 0$)[2,3]. (V_a denotes the volume of the air layer.)

1.3 Persistence

Aside from mechanical stability, the durability of an air layer around a solid object is to a high degree controlled by the exchange of "air" molecules between the air layer and – via diffusion through the surrounding water – the atmosphere. The Young-Laplace-Equation, Henry's Law

$$p_a = k_H c_a , \quad p_{atm} = k_H c_{atm} , \qquad (4)$$

and Fick's Law of diffusion

$$\boldsymbol{j} = -D_a \operatorname{grad} c , \qquad (5)$$

allow to derive the also intuitively plausible criterion $p_a \approx p_{atm}$ for the persistence of an air layer of pressure p_a which is in diffusional exchange with the atmosphere (pressure p_{atm}). Henry's Law states a proportionality between the mole fractions c_a (resp. c_{atm}) of air in water and the pressure p_a (resp. p_{atm}) of the air on the other side of the liquid/gas interface. k_H is Henry's Law constant. $\boldsymbol{j}$ denotes the flux of air molecules diffusing through water and D_a denotes the accordant constant of diffusion. Obviously, the air layer disappears if $p_a > p_{atm}$ lasts sufficiently long, and it grows whenever $p_a < p_{atm}$ is realised.

A systematic description of shape, stability and persistence of an air-water interface (resp. an air layer) which adheres to a given solid support would ideally start with solving the boundary value problem represented by Eq. (2) for $u(x,y)$. The result would allow to calculate the gas volume V, the mean curvature H and then – via Eqs. (1) and (3) – the quantity Ψ which is related to mechanical stability. Finally, the criterion $p_a \approx p_{atm}$ for the temporal persistence of the air layer could be assessed. This direct approach often fails at the first step, since Eq. (2) can rarely be solved explicitly.

More often, however, it is possible to establish the existence (or nonexistence) of a solution without actually calculating it. Similarly, moderate complex interface/solid configurations allow sometimes to assess whether a given air layer is also mechanically stable and persistent or not.

In what follows we will demonstrate in more detail this approach of combining exact information about existence, stability and persistence with approximate knowledge about the shape of an interface. In the next section we present a few intermediate results exhibiting a certain generality. Then we apply these results to specific examples.

2 Intermediate results

2.1 Shape, curvature and existence

We consider a regular lattice-like arrangement of vertical pillars with constant cross section standing on a

horizontal solid flat plane. We assume that an interface has formed stretching from pillar to pillar like a tent's roof.

We would like to know whether solutions of Eq. (2) exist if we prescribe the geometry of the (2D) unit cell of the lattice, the pillar radius and the contact angle between pillar and interface. Due to the symmetry of the situation it is sufficient to consider just one unit cell (see Fig. 2). Focussing on a single unit cell, the boundary condition consists of two parts: along the contact line of pillar and interface the contact angle θ can be arbitrarily prescribed, along the borders of the unit cells it has the value $\theta = \pi/2$ because otherwise, the symmetry of the situation would not allow a smooth interface.

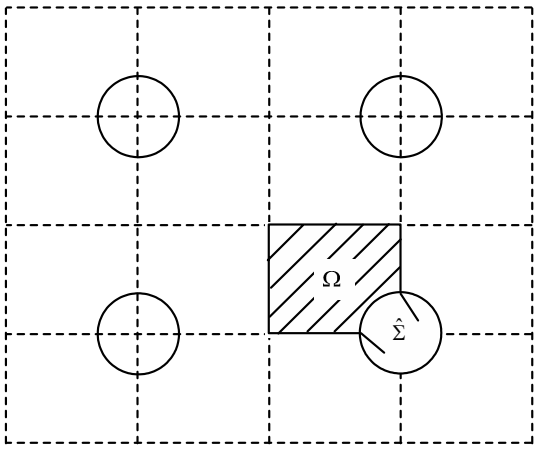

Fig. 2 Lattice-like arrangement of vertical pillars with constant cross section (solid circles) seen from above. The domain Ω (hatched region, area |Ω|) borders the pillar along $\hat{\Sigma}$. (In the situation depicted, the length $|\hat{\Sigma}|$ amounts to a quarter of the pillar's circumference.)

Application of the 2D divergence theorem yields a relation between mean curvature, contact angle and geometry of the elementary cell

$$H = \frac{\cos\theta\,|\hat{\Sigma}|}{2\,|\Omega|} \quad . \tag{6}$$

It is possible to derive a necessary and sufficient criterion[4,5] for the existence of a solution of the boundary value problem just described. Starting from the divergence theorem one performs a variety of manipulations and obtains eventually a scheme consisting of two steps.

Step 1: Try to inscribe into the domain Ω a (circular) arc Γ of radius

$$R_\theta = \frac{|\Omega|}{|\hat{\Sigma}||\cos\theta|} \tag{7}$$

which fulfills two conditions (see Figs. 2 and 3): (i) the angle between arc and $\hat{\Sigma}$ equals the contact angle θ, (ii) the angle between arc and any other boundary of Ω is 90°.

If this proves to be impossible, an interface $u(x,y)$ (i.e. a solution of Eq. (2)) which spans across the lattice characterised by the geometry Ω and $\hat{\Sigma}$ and forms a contact angle θ with the pillars does exist.

If it is possible to inscribe such an arc Γ into Ω, proceed to Step 2 to resolve the question of existence.

Step 2: The arc Γ cuts both the domain Ω and the contact line $\hat{\Sigma}$ into two pieces (for the definitions used in what follows consult Fig. 4). Calculate the functional

$$\Phi[\Gamma] = |\Gamma| - |\hat{\Sigma}^*|\cos\gamma + \frac{|\hat{\Sigma}|\cos\gamma}{|\Omega|}|\Omega^*| \tag{8}$$

for every arc Γ which could be inscribed into Ω in Step 1. If $\Phi[\Gamma] > 0$ for all arcs Γ related to the same boundary conditions a solution $u(x,y)$ of Eq. (2) under these boundary conditions exists. If one obtains $\Phi[\Gamma] \le 0$ for at least one of these arcs, no solution (i.e. no interface) exists.

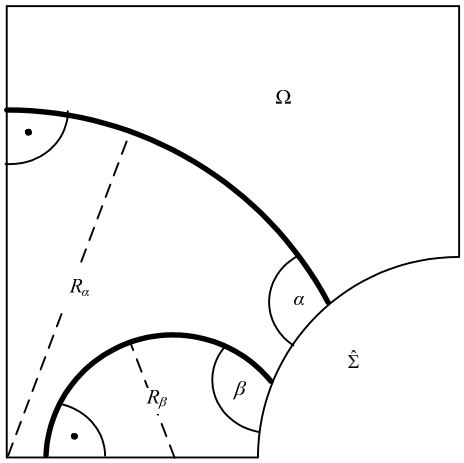

Fig. 3 Two circular arcs ($\theta = \alpha$ resp. $\theta = \beta$) satisfying the conditions of Step 1.

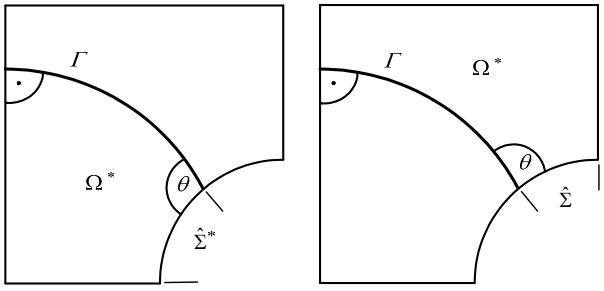

Fig. 4 Left: $\theta > \pi/2$, Right: $\theta < \pi/2$.

2.2 Persistence

We consider the situation depicted in Fig. 5. A spherical interface of radius ε containing air of pressure p_a is submersed in water at depth h below a flat water surface, above which the atmosphere (under air pressure p_{atm}) resides. Clearly, for

$$p_a \le p_{atm} \quad \text{(“Persistence condition”)}, \quad (9)$$

the submersed air bubble persists; whereas for $p_a > p_{atm}$, it will have disappeared after some time τ.

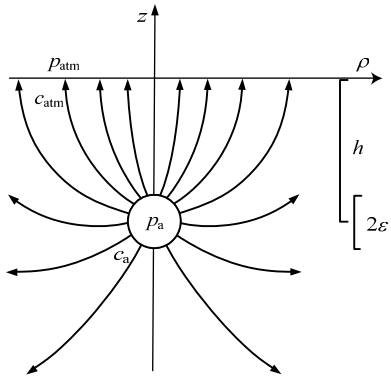

Fig. 5 Air bubble (radius ε, pressure p_a, depth h) in diffusional contact with the atmosphere (pressure p_{atm}). For $c_a > c_{atm}$ (equivalent to $p_a > p_{atm}$), air particles leave the bubble and diffuse along the trajectories ending in arrowheads towards the atmosphere.

2.2.1 Persistent bubble and submersion depth

Since the overlying water body contributes to the pressure within the bubble according to

$$p_w = p_{atm} + \rho_w g h , \quad (10)$$

(ρ_w denotes the density of liquid water, g the gravitational acceleration), it depends on the submersion depth h whether the bubble persists or dissolves. Insertion of Eq. (10) into Eq. (1) produces a criterion for the submersion depth h: persistence requires that h fulfills the condition

$$h < -\frac{2\sigma H}{\rho_w g} = h_\infty . \quad (11)$$

We call h_∞ the maximum persistence depth. If the air holding structure fulfills the assumptions leading to Eq. (6) (i.e. a lattice-like arrangement of vertical pillars with constant cross section standing on a horizontal solid flat plane) we may insert Eq. (6) into Eq. (11) and arrive at

$$h_\infty = -\frac{\sigma \cos\theta \, |\hat{\Sigma}|}{\rho_w g \, |\Omega|} . \quad (12)$$

It implies immediately that interfaces which attach to hydrophilic surfaces (which are characterised by a contact angle $0 < \theta < \pi/2$, leading to positive values of $\cos\theta$) can not persist.

2.2.2 Non-persistent bubble and lifetime

A bubble which violates the persistence condition Eq. (9) (or, equivalently, Eq. (11)) will vanish after a time τ. We now calculate τ if the pressures p_a and p_{atm}, the air bubble radius ε, its depth h and its air particle content n_a are prescribed.

First, we use Henry’s Law to obtain the associated mole fractions c_a and c_{atm} via Eq. (4). They are a prerequisite for the formulation of a boundary value problem for the diffusion equation

$$\frac{\partial c}{\partial t} = D_a \Delta c , \quad (13)$$

whose solution provides via Fick’s Law the flux $\boldsymbol{j}$ of air particles. Integration of $\boldsymbol{j}$ across the water/atmosphere interface gives the total air current I. Assuming temporal constancy of I (i.e. ignoring that during the first phase of diffusional transport particles have already left the bubble but no particles have yet arrived at the atmospheric interface), the lifetime τ of the submersed air bubble follows eventually from

$$\tau = \frac{n_a}{I} . \quad (14)$$

Neglecting “switch-on” effects implies that this expression underestimates the real bubble lifetime. Put differently, τ represents a lower boundary for bubble lifetime. Another implication of ignoring “switch-on” effects is that it suffices to consider the time-independent version of Eq. (13),

$$0 = D_a \Delta c . \quad (15)$$

Appropriate boundary conditions for this equation are (i) at the water/atmosphere interface

$$c|_{z=0} = c_{atm} , \quad (16)$$

and (ii) at the water/air boundary of the submersed bubble

$$c|_{\sqrt{\rho^2+(z+h)^2}=\varepsilon} = c_a . \quad (17)$$

Exploiting the axial symmetry of the situation we move to cylindrical coordinates (ρ, φ, z), where

$$\rho = \sqrt{x^2 + y^2} ,$$

represents the distance from the z-axis, and ϕ denotes the angle of rotation around it. An appropriate solution for the problem of Eqs. (15), (16) and (17) is given by the function[6]

$$c(\rho,z)=c_{\text{atm}}+\frac{\varepsilon(c_{\text{a}}-c_{\text{atm}})}{\sqrt{\rho^2+(z+h)^2}}-\frac{\varepsilon\,|\,(c_{\text{a}}-c_{\text{atm}})\,|}{\sqrt{\rho^2+(z-h)^2}}. \quad (18)$$

It satisfies Eqs. (15) and (16) exactly and (17) in good approximation provided $\varepsilon/2h \ll 1$. This is realised if the air retaining structures of the submersed object are small compared to the submersion depth. Notice that ε is assumed to represent half the maximum length of these structures.

Upon insertion of Eq. (18) into Eq. (5) we find

$$\boldsymbol{j}\,|_{z=0}=2\varepsilon h D_{\text{a}}\frac{(c_{\text{a}}-c_{\text{atm}})}{\sqrt{\rho^2+h^2}^3}\ . \quad (19)$$

Integration over the xy-plane (i.e. the water/atmosphere interface) yields

$$I=2\varepsilon h D_{\text{a}}(c_{\text{a}}-c_{\text{atm}})\int_{\rho=0}^{\infty}\int_{\phi=0}^{2\pi}\frac{d\phi\rho d\rho}{\sqrt{\rho^2+h^2}^3}$$
$$=4\pi\varepsilon D_{\text{a}}(c_{\text{a}}-c_{\text{atm}}). \quad (20)$$

Combining Eqs. (14), (4) and (20) with the Gas Equation $p_{\text{a}}V_{\text{a}}=n_{\text{a}}RT$ we obtain for the bubble lifetime

$$\tau=\frac{p_{\text{a}}V_{\text{a}}k_H}{4\pi\varepsilon D_{\text{a}}RT(p_{\text{a}}-p_{\text{atm}})}\ , \quad (21)$$

where R and T are the gas constant and temperature, respectively.

Noting that at depth h the water pressure p_{w} splits up according to $p_{\text{w}}=p_{\text{atm}}+\rho_{\text{w}}gh$, we insert Eq. (1) into Eq. (21) and get

$$\tau=\frac{V_{\text{a}}k_{\text{H}}}{4\pi\varepsilon D_{\text{a}}RT}\left(1+\frac{p_{\text{atm}}}{\rho_{\text{w}}gh+2\sigma H}\right). \quad (22)$$

Replacing H in favour of h_∞ (defined in Eq. (11)) we obtain for the bubble lifetime (or at least its lower boundary) the overall result

$$\tau=\begin{cases}\infty & \text{if } h\le h_\infty\\ \dfrac{V_{\text{a}}k_{\text{H}}}{4\pi\varepsilon D_{\text{a}}RT}\left(1+\dfrac{p_{\text{atm}}}{\rho_{\text{w}}g(h-h_\infty)}\right) & \text{if } h>h_\infty\end{cases}. \quad (23)$$

The validity of Eq. (23) is not restricted to $h_\infty > 0$. Although the descriptive meaning of the term "maximum persistence depth" is obvious only for $\pi/2 < \theta < \pi$, the mathematical machinery behind Eqs. (9), (11) and (23) works fine also if the contact angle is in the interval $0 < \theta < \pi/2$.

3 Examples

We consider two specific examples which have in common a lattice-like arrangement of vertical pillars with constant cross section standing on a horizontal solid flat plane. In one case, the pillars form a (2D) cubic lattice, and in the other case, a hexagonal lattice (see Fig. 6). It is to be expected that in both cases an interface stretches from pillar to pillar like a tent's roof, similar to that in Fig. 7 which represents already an abstraction of the leaf surface of the floating fern *Salvinia*[7].

In what follows we shall need the unit cell area $|\Omega|$ and the contact line length $|\hat{\Sigma}|$ associated with it expressed in terms of the lattice constant a and the pillar radius r. They are

Hexagonal lattice

$$|\Omega|=\frac{\sqrt{3}a^2-2\pi r^2}{12},\quad |\hat{\Sigma}|=\frac{\pi r}{3}\ , \quad (24)$$

Cubic lattice

$$|\Omega|=\frac{a^2-\pi r^2}{4},\quad |\hat{\Sigma}|=\frac{\pi r}{2}\ . \quad (25)$$

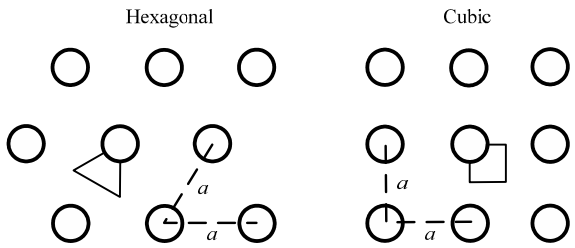

Fig. 6 Hexagonal (left) and cubic (right) lattice of vertical pillars seen from above. a denotes the lattice constant. The polygons in the centres outline the unit cell of the respective lattice.

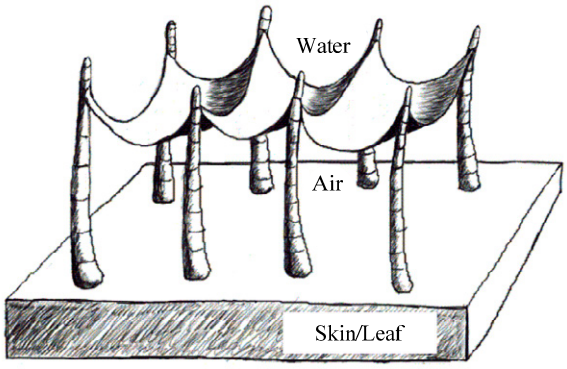

Fig. 7 The surface of the floating fern *Salvinia* is enclosed by an air layer whose outer interface stretches between pillarlike protrusions, resembling a tent's roof.

3.1 Shape and Existence

Applying the existence criterion described in Section **2.1** we find that for a hexagonal lattice an interface exists for all values of the contact angle θ, the lattice constant a and the pillar radius r (provided $a \geq 2r$ is satisfied). In the case of the cubic lattice, however, there are combinations of θ and a/r which allow no solution (see Fig. 8).

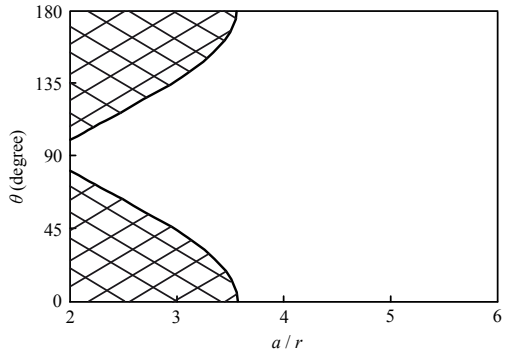

Fig. 8 Area of existence of an interface attached to round pillars arranged in a 2D cubic lattice. The lattice constant a is given in multiples of the pillar radius r, thus $a \geq 2r$, θ is contact angle. No solution exists for the (a / r, θ)-pairs in the hatched regions of the (a / r, θ)-plane.

3.2 Stability

Combining Eqs. (6) and (24) (resp. Eq. (25)) one sees that the curvature H of the interface $u(x,y)$ depends only on the area of the unit cell (defined by the parameters a and r) but not on the thickness of the air layer. Thus, the quantity Eq. (3) reduces to

$$\psi = \left[\frac{p_a}{V_a} \right]_0 > 0 \ , \qquad (26)$$

i.e. the interface is stable against (small) mechanical perturbations.

3.3 Persistence

Application of Eq. (12) for the maximum persistence depth h_∞ as function of the lattice constant a produces Fig. 9. Obviously, increasing the distances between the pillars (i.e. increasing the lattice parameter a) decreases the depth h_∞ within which submersed air bubbles do not peter out. Furthermore, the contact angle (pairs of solid and broken curves correspond to $\theta = 95^\circ$, 120°, 160°) has a greater effect on h_∞ than the arrangement of the pillars (solid lines: cubic lattice, broken lines: hexagonal lattice). Notice that the curves corresponding to the cubic lattice and to the contact angles $\theta = 120^\circ$ and $\theta = 160^\circ$ exist only for $a \gtrapprox 13$ μm and $a \gtrapprox 17$ μm (see Fig. 8), respectively, if the pillars have radius $r = 5$ μm.

Air bubbles which are deeper submersed than h_∞ disappear after a time τ, according to Eq. (23). Fig. 10 depicts the dependence of τ on the difference $h - h_\infty$ for an air volume $V_a = b_1\, b_2\, l$. b_1 and b_2 denote the side lengths of the rectangular solid plane on which the pillars are erected, l denotes the (averaged) initial thickness of the air layer. The radius ε which appears in the derivation of τ in section **2.2** follows from equating the interface area $b_1 b_2$ with the surface area $4\pi\varepsilon^2$ of a sphere with radius ε.

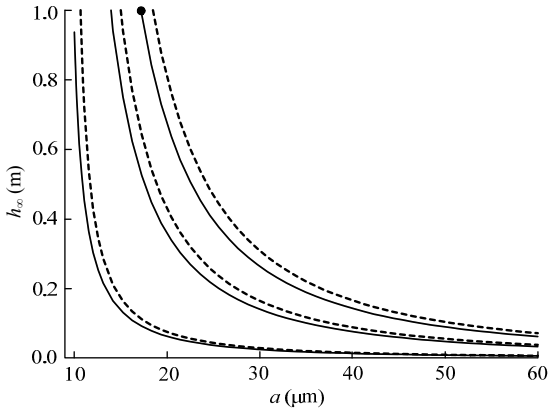

Fig. 9 Maximum persistence depth h_∞ as function of the lattice constant a for $r = 5$ μm (see Eq. (12)). Solid and broken lines are related to the cubic and hexagonal lattices depicted in Fig. 2. The pairs of curves correspond to the contact angles $\theta = 95^\circ$ (closest to axes), $\theta = 120^\circ$ (central) and $\theta = 160^\circ$.

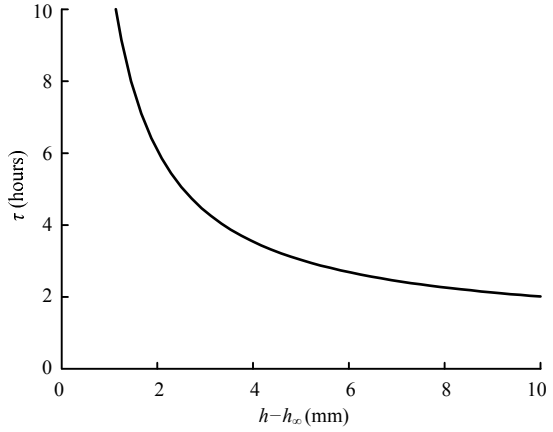

Fig. 10 Lifetime τ of an submersed air bubble as function of the difference $h - h_\infty$ according to Eq. (23). Input values: $T = 293$ K, $V_a = b_1 b_2 l$ with $l = 30$ μm, $b_1 = 18$ mm, $b_2 = 13.5$ mm.

4 Conclusions

We have demonstrated that fundamental properties of air-water interfaces attached to pillars which are arranged as 2D lattices can be deduced without solving

explicitly the differential equation which governs the shape of such interfaces. Efforts to devise submersed objects, which are able to develop air layers with prescribed behaviour with respect to stability and persistence, may benefit from this approach.

In the future we will expand two aspects of our approach.

(i) At first sight, Eq. (26) predicting stability of interfaces attached to arbitrarily wide lattices seems to contradict common sense. However, Eq. (26) rests on the assumption of small deflexions of an interface from its equilibrium position. Thus, we presume that an improved stability criterion, which compares various formation energies quantitatively (and is therefore not restricted to small perturbations), will remedy this defect.

(ii) So far we examined air layers which are attached to pillars of constant radius and constant contact angle. According to section **2.2** such air layers show a very delicate behaviour with respect to persistence: at any submersion depth other than h_∞ (defined in Eq. (12)) they necessarily lose or accumulate air molecules. This rigid coupling between persistence and the properties of the solid, to which the air layer attaches, is a direct consequence of the constancy of pillar radius and contact angle. Hence, it appears worthwhile to extend our approach to (a) pillars of non-constant radius (e.g. cones), (b) pillars with varying contact angle, and (c) flexible pillars. First results indicate that such pillars may lead to the formation of air layers which are both stable and persistent at a wide range of submersion depths.

Acknowledgments

Parts of this work were funded by grants from the Deutsche Forschungsgemeinschaft, the Bundesministerium für Bildung und Forschung and the Landesgraduiertenförderungsgesetz des Landes Baden-Württemberg, which are gratefully acknowledged. We thank Birgit Binder, Tübingen, for contributing Figs. 1 and 7.

References

[1] Atkins P. *Physical Chemistry*, W H Freeman, New York, 1998.

[2] Shen F, Gao R, Liu W, Zhang W. Physical analysis of the process of cavitation in xylem sap. *Tree Physiology*, 2002, **22**, 655–659.

[3] Konrad W, Roth-Nebelsick A. The significance of pit shape for hydraulic isolation of embolized conduits of vascular plants during novel refilling. *Journal of Biological Physics*, 2005, **31**, 57–71.

[4] Finn R. *Equilibrium Capillary Surfaces. Grundlehren der mathematischen Wissenschaft*, 284, Springer-Verlag, New York, 1985.

[5] Giusti E. Boundary value problems for non parametric surfaces of prescribed mean curvature. *Annali della Scuola Normale Superiore di Pisa*, *Classe di Scienze* 4, 1976, **3**, 501–548.

[6] Arfken G. *Mathematical Methods for Physicists*, Academic Press, New York, 1970.

[7] Barthlott W, Wiersch S, Colic Z, Koch K. Classification of trichome types within the water ferns Salvinia and ontogeny of the egg-beater trichomes. *Botany*, 2009, **87**, 830–836.